

Cohesive zone modeling of thin aluminium sheets

O.S. Vishnu, Mahendra Gattu^a

^aDepartment of Civil Engineering, National Institute of Technology, Rourkela, 769008, India.

Abstract

Single edge notch (SEN) aluminium specimens of widths (D): 20, 40 and 50mm are tested under uniaxial tensile loading for a strain rate of 0.005/minute. The notch depth to width ratio ($a/D=0.25$) and the gauge length to width ratio ($L/D=2.5$) are constant for these tested specimens. The load versus deflection curves are analyzed using cohesive crack model. The peak stress data are analyzed using equivalent elastic crack model. The fracture energy G_f obtained from these approaches are compared. Uniaxial tensile testing of 50mm width SEN specimens ($L/D=2.5$) with ligament lengths of 2.5, 5, 7.5, 10, 12.5 and 15mm is carried out. A linear regression fit between work of fracture per unit ligament area and ligament length is used to determine the essential work of fracture. An energy based approach involving fixed point iteration method to calculate the crack length at peak load is proposed.

[copyright information to be updated in production process]

Keywords: Aluminium; Plane Stress; Cohesive-zone; Fracture Toughness; Essential-work-of-fracture; R-curve

1. Introduction

The main objective of the research described in this article is to examine the fracture behavior of aluminium sheets under plane stress conditions from different theoretical perspectives. Mode-I tensile testing of thin aluminium sheets is carried out. The experimental data is analyzed using equivalent elastic crack model and cohesive zone model. The mode-I plane stress fracture toughness K_{Ic} determined using these two approaches is compared.

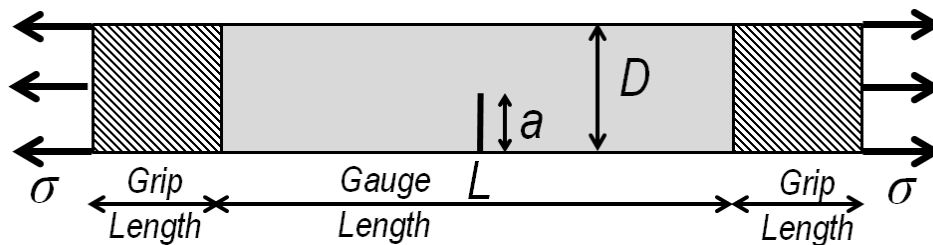


Fig. 1: Test Geometry

1.1. Test geometry

Test specimens made of pure aluminium are prepared. The typical geometry of the test specimens is shown in figure 1. The dimensions of the test specimens are listed in table 1.

Table 1. Geometry of test specimens.

Depth, <i>D</i> (mm)	Length, <i>L</i> (mm)	Notch Depth, <i>a</i> (mm)	Number of Samples
20	50	0	3
40	100	0	3
50	125	0	3
20	50	5	3
40	100	10	3
50	125	12.5	3

All specimens are tested at a strain rate of 0.25 mm/minute. The peak stress values are calculated. The load *P* versus deflection *u* curves are determined for all the specimens.

1.2. Peak Stress and Work of Fracture Data

The load deflection curves indicates the ductile behavior of thin aluminium sheets. The peak stress values and work of fracture values are listed in table 2.

Table 2. Peak stress values of test specimensS

Depth, <i>D</i> (mm)	Notch Depth, <i>a</i> (mm)	Peak Stress (N/mm ²)	WOF (N.m/m ²)
20	5	99.81, 91.80, 90.64	128.8, 111.9, 119.5
40	10	90.54, 89.78, 90.38	144.6, 170.5, 152.5
50	12.5	90.02, 93.77, 92.05	232.5, 285.5, 269.5

2. Equivalent Elastic Crack Model

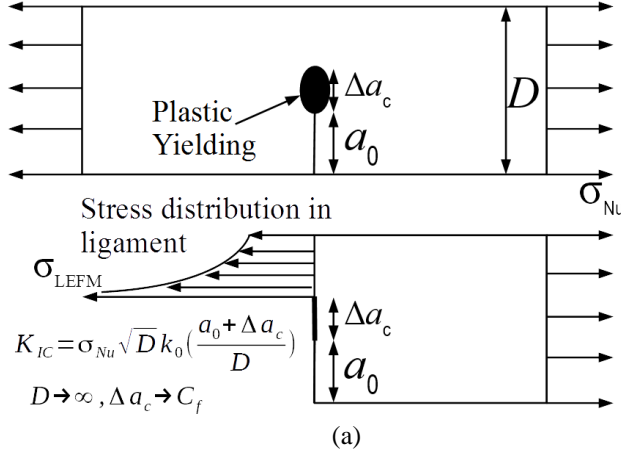
2.1. Linear regression Analysis

The pictorial representation of equivalent elastic crack model is shown in figure 2. The fracture process zone at the crack tip is almost entirely occupied by the plastic zone. To apply linear elastic fracture mechanics concepts, plastic zone is lumped into a line of length Δa_c . As size $D \rightarrow \infty, \Delta a_c \rightarrow C_f$. The fracture toughness is given by the equation:

$$K_{Ic} = \sigma_{Nu} \sqrt{D} k_o \left(\alpha_o + \frac{C_f}{D} \right),$$

$$\alpha_o = \frac{a_0}{D}.$$

Using Taylor's series expansion, three equations can be obtained as show in figure 2. The fracture toughness K_{Ic} and C_f for the three linear regression equations are given in table 3 and in figure 3. The K_{Ic} value predicted by linear regression 3 equation differs by 50% as compared with linear regression equations 1 and 2. To predict the correct value, a crack growth resistance curve approach is examined.



$$k_0 = k_0(\alpha_0), \quad k'_0 = k'_0(\alpha_0)$$

$$K_{1c}^2 = \sigma_{Nu}^2 D k_0^2 \left(\alpha_0 + \frac{C_f}{D} \right) = \sigma_{Nu}^2 D \left(k_0^2 + 2k'_0 k_0 \frac{C_f}{D} \right)$$

$$\text{Linear Regression 1: } \frac{1}{\sigma_{Nu}^2} = \frac{k_0^2}{K_{1c}^2} D + \frac{2k'_0 k_0}{K_{1c}^2} C_f$$

$$\text{Linear Regression 2: } \frac{1}{\sigma_{Nu}^2 D} = \frac{2k'_0 k_0 C_f}{K_{1c}^2} \frac{1}{D} + \frac{k_0^2}{K_{1c}^2}$$

$$K_{1c} = \sigma_{Nu} \sqrt{D} k_0 \left(\alpha_0 + \frac{C_f}{D} \right) = \sigma_{Nu} \sqrt{D} \left(k_0 + k'_0 \frac{C_f}{D} \right)$$

$$\text{Linear Regression 3: } \frac{1}{\sigma_{Nu} \sqrt{D}} = \frac{k'_0 C_f}{K_{1c}} \frac{1}{D} + \frac{k_0}{K_{1c}}$$

Figure 2: Equivalent Elastic Crack Model

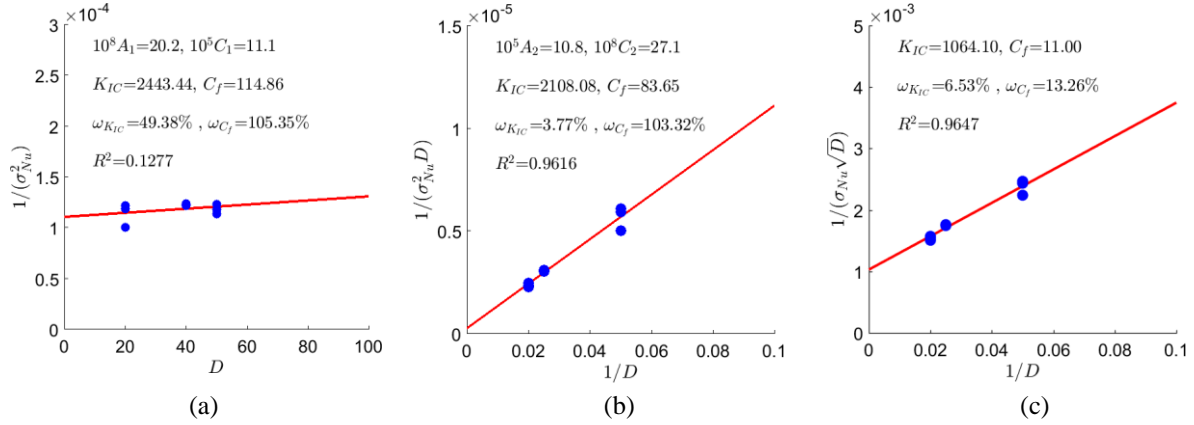


Figure 3: Linear regression analysis

Table 3. Fracture Parameters obtained from equivalent elastic crack model.

Linear Regression Equation	K_{Ic}	C_f	G_f
1	2443	114.9	148.9
2	2108	83.7	110.9
3	1064	11.0	28.3

2.2. Crack growth resistance curve

The crack growth resistance curve i.e. R-curve is obtained from the experimental data. The strain energy term

$G_u(\sigma_{Nu}^{(i)}, D^{(i)}, \Delta a^{(i)})$, is given by the equation $G_u = \frac{(\sigma_{Nu}^{(i)})^2 D^{(i)}}{E_i} k_0^2 \left(\alpha_0 + \frac{\Delta a^{(i)}}{D^{(i)}} \right)$, $i=1,2,3$ is for three different sizes $D^{(i)}$ = 20, 40, 50, $\sigma_{Nu}^{(i)}$ is average of the peak stress value and E_i is the average Youngs Modulus for size D_i specimens.

The R-curve given by $R(\Delta a)$ satisfies two conditions: 1. $R(\Delta a_c^i) = G_u(\sigma_{Nu}^i, D^i, \Delta a_c^i)$, 2. $\frac{\partial R}{\partial \Delta a} = \frac{\partial G_u}{\partial \Delta a}$

The function form of R-curve is assumed as $R = \beta^{peak} (1 - \exp(-\gamma \Delta a))$. The parameters β^{peak} and γ are determined numerically using Levenberg-Marquardt algorithm. The details of the algorithm are given in reference[1]. Figure 4 shows the R-curve and table 4 shows the results of the R-curve.

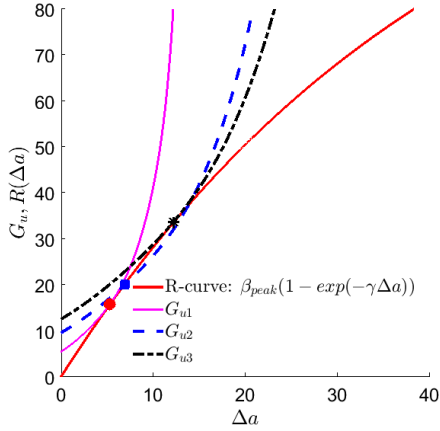


Figure 4: Crack growth resistance curve

Table 4. Fracture Parameters obtained from R-curve approach

Size	Δa_c	$R(\Delta a_c)$	K_{Ic}
20	5.32	15.78	785
40	6.92	20.17	902
50	12.29	33.69	1170

3. Cohesive Zone model

3.1. Finite element simulation of load versus deflection curve using cohesive zone model

In elastic plastic fracture mechanics, the plastic zone at the crack tip can be assumed to have uniform yield stress σ_Y . This model was proposed by Dugdale. Barenblatt[2] proposed a model where the stress in the plastic zone is non-uniform and varies with the crack opening. This model inspired the used of cohesive zone modelling to model the stresses in the plastic zone developed at the crack tip. A traction separation curve relates the crack opening w with the cohesive stress $\sigma(w)$. Depending on the material, different traction separation laws have been proposed. For quasi-brittle materials like concrete, linear, bi-linear and exponential traction separation laws are proposed in literature[3]. In this study, we propose a traction separation law as indicated in figure. The four parameters are f_t^0, f_t^1, w_0, w_1 with $f_t^1 = f_t^0$.

The geometry of the finite element model is shown in the figure. A 4-node quadrilateral element of mesh size 1×1 unit is used. The initial young's modulus $E_{initial}$ is calculated for each sample from its load deflection curve and this value is used as elastic modulus E_{FEM} in the finite element model simulating the load versus deflection curve of the specific sample.

The nodes in the ligament region are freed one node at a time. The freed nodes follow traction-separation law. The corresponding displacement u_0 and the axial force P_0 is calculated using Petersson's influence function method. After all the nodes are freed, the displacement are increased gradually until the specimen fails completely. The experimental load versus deflection curves are fit using the parameters of this model $f_t^0 = f_t^1 = 121, w_0 = 2 * 0.7, w_1 = 2 * 0.154$: as shown in figure. The fracture energy G_f is determined as $G_f = 0.5 f_t^0 w_1 + 0.5 f_t^1 w_0 = 103.3 \text{ Nm/m}^2$. The value of $f_t^0 w_1 = 37.27 \text{ Nm/m}^2$.

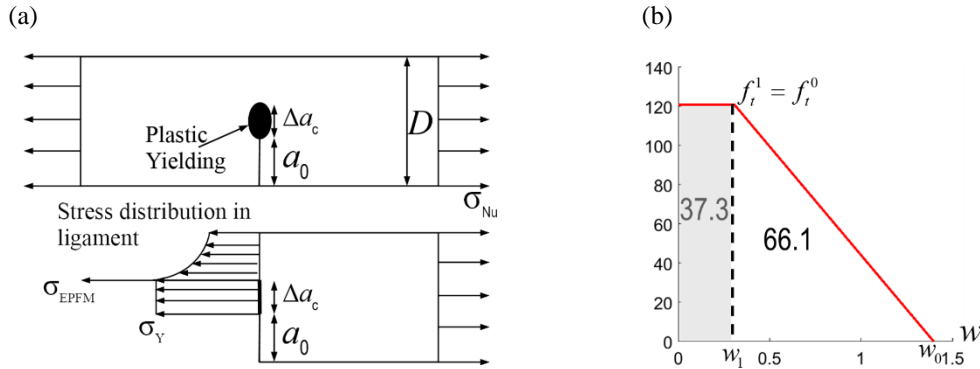


Figure 5 a) Elastic-Plastic fracture mechanics: Dugdale model b) Cohesive zone Model: Traction Separation Law

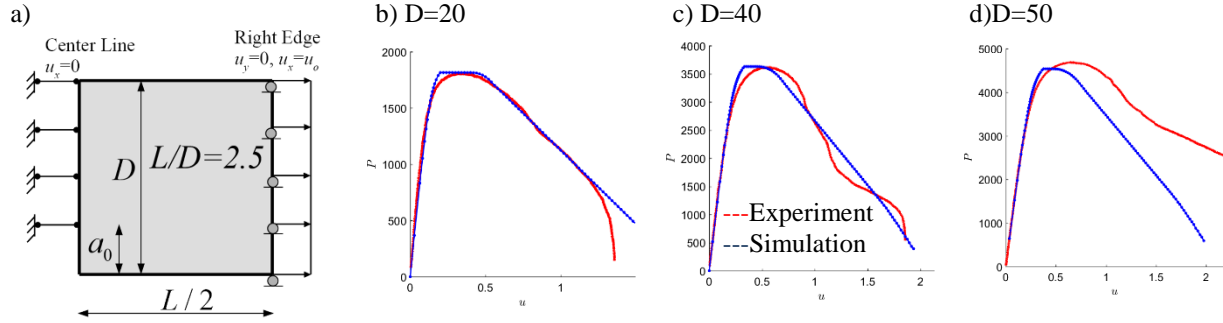


Figure 6 a) Geometry of Finite Element Model, b), c), d) : Load-deflection curves experimental vs simulation

4. Essential work of fracture

4.1. Description of experiments

The total area under load deflection curve gives the energy required to break the specimen into two pieces. It is also known as work of fracture (WOF). This area divided by the ligament area gives fracture energy G_F . A part of the energy is used to create new crack surface (essential work of fracture) and another part is dissipated as plastic deformation work in the plastic zone at the crack tip. To determine this essential work of fracture, we test specimens of geometries with constant depth $D=50$ mm and varying ligament lengths ($D-a$): 2.5 mm, 5.0 mm, 7.5 mm, 10 mm, 12.5 mm and 15 mm. Three samples are tested for each geometry resulting in a total of 18 test specimens. The load P versus deflection u curves are obtained. The peak stress data are calculated.

4.2. Determining essential work of fracture

A known linear relationship between work of fracture per unit ligament area and ligament length exists in literature([4],[5], [6]) given as $\frac{WOF}{(D-a)t} = w_e + \beta w_p(D-a)$. w_e is essential work of fracture and βw_p gives the plastic work done. From the 18 WOF values, a linear regression fit gives the values of $w_e = 115.8$ N.m/m² and $\beta w_p = 5.76$ N.m/m² as shown in figure 7(b) .

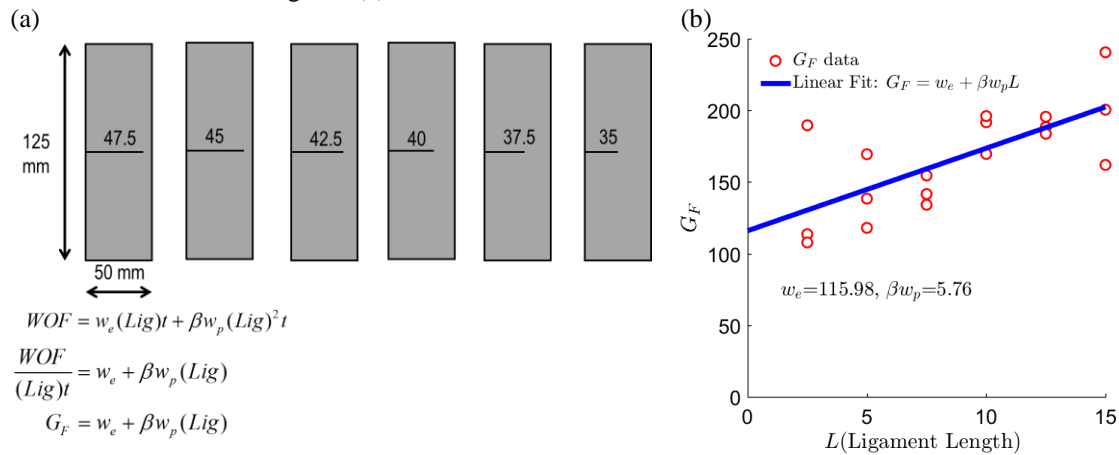
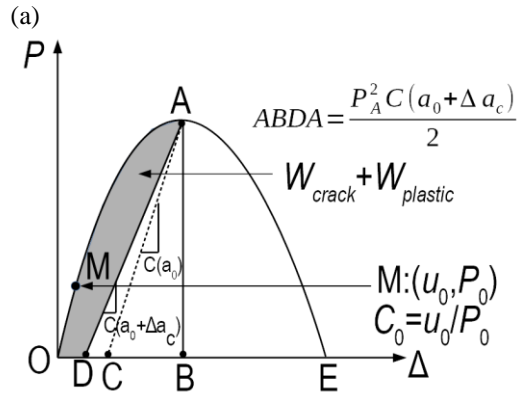


Figure 7 (a) : Test geometries (b) Linear fit to determine essential work of fracture

4.3. Fixed point iteration algorithm to calculate crack length at peak load

An algorithm to calculate the crack length at peak load is proposed in figure 8. The results of this approach are given in table 5.



(b)

$$OADO = OABO - ADBA$$

$$ADBA = 0.5P_A^2 C(a_0 + \Delta a_c)$$

$$C(a_0 + \Delta a_c) = \frac{C_0 \Psi\left(\frac{a_0 + \Delta a_c}{d}\right)}{\Psi\left(\frac{a_0}{d}\right)}$$

C_0 : Initial compliance
 $\Psi(a)$: Compliance function of normalized notch depth

$$OADO = OABO - 0.5P_A^2 \frac{C_0 \Psi\left(\frac{a_0 + \Delta a_c}{d}\right)}{\Psi\left(\frac{a_0}{d}\right)}$$

(c)

$$OADO = W_{crack} + W_{plastic}$$

$$W_{plastic} = \frac{4 K_I^2}{\pi E} t \Delta a_c$$

$$K_I = \sigma_{Nu} \sqrt{D} k_0 \left(\alpha_0 + \frac{\Delta a_c}{D} \right)$$

$$\alpha_0 = a_0 / D$$

$$W_{plastic} = \frac{4 \sigma_{Nu}^2 D}{\pi E} \left[k_0 \left(\alpha_0 + \frac{\Delta a_c}{D} \right) \right]^2 t \Delta a_c$$

$$W_{crack} = w_e t \Delta a_c$$

$$OADO = w_e t \Delta a_c + \frac{4 \sigma_{Nu}^2 D}{\pi E} \left[k_0 \left(\alpha_0 + \frac{\Delta a_c}{D} \right) \right]^2 t \Delta a_c$$

(d)

Equating OADO

$$OABO - 0.5P_A^2 \frac{C_0 \Psi\left(\frac{a_0 + \Delta a_c}{d}\right)}{\Psi\left(\frac{a_0}{d}\right)} = w_e t \Delta a_c + \frac{4 \sigma_{Nu}^2 D}{\pi E} \left[k_0 \left(\alpha_0 + \frac{\Delta a_c}{D} \right) \right]^2 t \Delta a_c$$

Solving for Δa_c using fixed point iteration

$$\Delta a_c = \frac{OABO - 0.5P_A^2 \frac{C_0 \Psi\left(\frac{a_0 + \Delta a_c}{d}\right)}{\Psi\left(\frac{a_0}{d}\right)}}{\left(w_e + \frac{4 \sigma_{Nu}^2 D}{\pi E} \left[k_0 \left(\alpha_0 + \frac{\Delta a_c}{D} \right) \right]^2 \right) t}$$

Figure 8 : Fixed point iteration algorithm to determine the crack length at peak load

Table 5. Fracture Parameters obtained from fixed point iteration algorithm

Size	Sample	Δa_c	E	K_{Ic}	G_f
20	1	3.63	37276	717.2	13.8
20	2	2.99	34709	620.9	11.11
20	3	2.38	36277	577.7	9.201
40	1	4.71	43427	814.3	15.27
40	2	6.29	46773	871.8	16.25
40	3	6.34	48111	879.7	16.09
50	1	8.02	46760	983.4	20.68
50	2	9.00	48132	1062	23.44
50	3	7.96	40839	1003	24.64

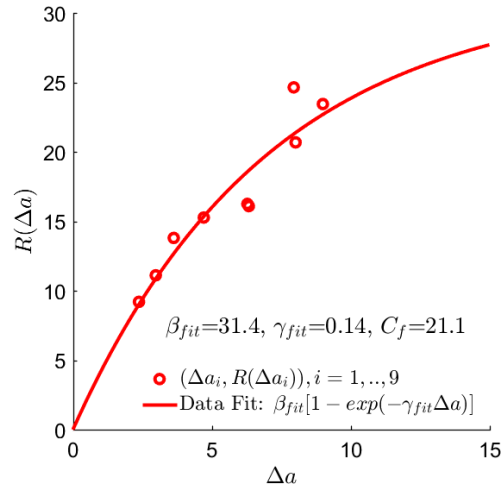


Figure 9: R-curve obtained from fixed point algorithm

A crack growth resistance curve can be obtained from the values of G_f and Δa_c calculated in table 5 and shown in figure 9a. The value of the parameters of R-curve $\beta_{fit}=31.4 \text{ Nm/m}^2$ and $C_f=21.1 \text{ mm}$. This value is comparable with the area under the initial part of the curve (37.3 N.m/m^2) in traction separation law shown in figure 5b.

5. Discussion

The fracture of aluminium sheets has been investigated using different theoretical approaches. Using the equivalent elastic crack model, the linear regression equations 1 and 2 gave G_f and C_f values which are 3-5 times higher than those obtained by linear regression 3. The cohesive zone model was able to capture the load versus deflection for size $D=20, 40$ samples. For $D=50$ samples, the post peak slope of the experiment was milder compared to the simulation. The fixed point iteration algorithm gives G_f value which agrees with the linear regression 3 of equivalent elastic crack model. The G_f calculated from the work of fracture and from equivalent elastic crack model (Linear Regression 1 and 2) are larger than the G_f obtained from essential work of fracture approach considering fracture behavior upto peak loads.

5.1. Modifying the Youngs modulus used in the G_f calculation.

In fixed point iteration algorithm, at peak load, we calculate $K_I = \sigma_{NU} \sqrt{D} k (\alpha_0 + \frac{\Delta a_c}{D})$. The material is at the peak state of loading and its stiffness is reduced considerably. As a result, the Youngs modulus E at peak load is no longer same as the initial Youngs modulus $E_{initial}$. The expression for fracture energy $G_f = \frac{K_I^2}{E}$ uses the initial Youngs modulus $E_{initial}$. This results in G_f which is significantly lower than the G_F obtained from work of fracture approach.

Using a Youngs modulus E smaller than the $E_{initial}$ will result in higher G_f values in the fixed point iteration algorithm. Then the results of G_f can match the G_F values obtained from work of fracture approach. This idea will have to be supported by a mathematical framework in future.

Acknowledgements

The authors thank the Department of Civil Engineering, National Institute of Technology, Rourkela, India for providing the necessary laboratory space and equipment to carry out the experiments.

References

- [1] A. Satyanarayana and M. Gattu, "Effect of displacement loading rates on mode-I fracture toughness of fiber glass-epoxy composite laminates," *Eng. Fract. Mech.*, vol. 218, no. July, p. 106535, 2019.
- [2] G. I. Barenblatt, "The Mathematical Theory of Equilibrium Cracks in Brittle Fracture," *Adv. Appl. Mech.*, vol. 7, no. C, pp. 55–129, 1962.
- [3] A. Hillerborg, M. Mod er, and P. E. Petersson, "Analysis of crack formation and crack growth in concrete by means of fracture mechanics and finite elements," *Cem. Concr. Res.*, vol. 6, no. 6, pp. 773–781, 1976.
- [4] B. Cotterell and J. K. Reddel, "The essential work of plane stress ductile fracture," *Int. J. Fract.*, vol. 13, no. 3, pp. 267–277, 1977.
- [5] K. Duan, X. Hu, and G. Stachowiak, "Modified essential work of fracture model for polymer fracture," *Compos. Sci. Technol.*, vol. 66, no. 16, pp. 3172–3178, 2006.
- [6] M. Y. Abdellah, "Essential work of fracture assessment for thin aluminium strips using finite element analysis," *Eng. Fract. Mech.*, vol. 179, pp. 190–202, 2017.